Noname manuscript No.
(will be inserted by the editor)

An Adaptive Energy Detection Scheme with Real-time Noise Variance Estimation

Libin K Mathew · Shreejith Shanker · A P Vinod · A S Madhukumar

Received: date / Accepted: date

Abstract Energy detection-based spectrum sensing techniques are ideally suited for power-constrained cognitive radio applications because of their lower computational complexity compared to feature detection techniques. However, their detection performance is dependent on multiple factors like accuracy of noise-variance estimation and signal to noise ratio (SNR). Many variations of energy detection techniques have been proposed to address these challenges; however they achieve the desired detection accuracy at the cost of increased computational complexity. This restricts the use of enhanced energy detection schemes in power-constrained applications such as aeronautical communication. In this paper, an adaptive low-complexity energy detection scheme is proposed for spectrum sensing in an L-band Digital Aeronautical Communication System (LDACS) at lower SNR levels. Our scheme uses a real time noise variance estimation technique using autocorrelation which is induced by the cyclic prefix property in LDACS signals. The proposed technique does not incur dedicated hardware blocks for noise variance estimation, leading to an efficient hardware implementation of the scheme without significant resource overheads. The simulation studies of the proposed scheme shows that the desired accuracy (90% detection accuracy with only 10% of false alarms) can be achieved even at -16.5 dB SNR, significantly lowering the SNR wall over existing energy detection schemes.

Key words: Cognitive radio, spectrum sensing, Energy detection, Noise variance estimation

Libin K Mathew* and A S Madhukumar**
Nanyang Technological University Singapore
E-mail: libin001@e.ntu.edu.sg*,asmadhukumar@ntu.edu.sg**

Shreejith Shanker
Trinity College Dublin, Ireland
E-mail: shankers@tcd.ie

A P Vinod
Indian Institute of Technology, Palakkad, Kerala,India
E-mail: vinod@iitpkd.ac.in

1 Introduction

Air traffic has seen tremendous development over the last two decades and is expected to double in capacity by 2025 [3]. On the other hand, air traffic management (ATM) systems are currently approaching operating limits especially in high-density areas and in the current form, ATMs will not be capable of handling the projected growth in future air traffic [9]. To address this challenge, the European Organization for the Safety of Air Navigation (EUROCONTROL) and the Federal Aviation Administration (FAA) is developing the Future Communications Infrastructure (FCI) that comprises current and future communication technologies. Two projects have been initiated to modernise the Air Traffic Management (ATM): the Next Generation Air Transportation System (NextGen) [1] in United States, and the Single European Sky ATM Research (SESAR) [27] in Europe. The International Civil Aviation Organization (ICAO) recommended the use of L-band (between 960 and 1164 MHz) for future aeronautical communication systems. The technology for future Air-to-Ground communication, LDACS (L-band Digital Aeronautical Communication System), uses an inlay approach with legacy L-band systems like Distance Measuring Equipment (DME). LDACS is proposed as a Frequency Division Duplexing (FDD) based system with Orthogonal Frequency Division Multiplexing (OFDM) as the modulation scheme [23].

Use of cognitive radio (CR) concepts has been proposed for LDACS to improve its spectral efficiency [11, 18, 25]. Like a traditional CR system, two types of communication are considered in the aeronautical scenario. A primary aircraft (or Primary User (PU)) has specific LDACS channels pre-allocated for communication between the aircraft and the ground station. The secondary aircraft (or Secondary User (SU)) uses dynamic spectrum access to detect (as use) vacant LDACS channels for communicating to the ground station in an opportunistic manner, without affecting the primary aircraft. Unlike terrestrial systems, spectrum sensing in LDACS offers unique challenges as channel conditions and signal quality can vary rapidly due to the non-stationary nature of aircrafts around a fixed ground station. Also, aircraft systems operate on limited energy budget and hence necessitates the use of low complexity spectrum sensing schemes to meet strict power consumption limitations. Though feature detection techniques like matched filtering and cyclostationary detection schemes offer better detection accuracy at low SNR regimes, high complexity and long sensing duration requirements of these techniques make it less attractive for aeronautical communications. Energy Detection (ED) based techniques are ideally suited for this scenario due to their low complexity and incoherent nature. However, conventional ED relies on accurate estimation of noise variance to meet performance requirements and also suffers from inability to distinguish between primary and other (malicious) users [5]. Also, detection accuracy of conventional ED deteriorates significantly at lower SNR regimes. While alternative forms of ED have been investigated to address these shortcomings, they achieve such improvements at the cost of much higher computational complexity and hence power consumption.

In this paper, an energy difference based Weighted Energy Averaging Scheme (WEAS) is proposed to reduce the effective variance of the test statistic and thereby lower the SNR wall with minimal computational overhead. The weighted sum of the current and the past energy values are considered as the test statistic in the proposed scheme. An energy-difference algorithm is proposed to detect

channel state changes, and is combined with the weighted averaging scheme with dynamically tuned weights to counter performance degradation issues. The energy-difference algorithm takes the difference of received signal energy from the current and the previous sensing slots and compares it with a predefined threshold for detecting state changes. The algorithm further tunes the weights for the energy values based on state change information and estimated noise variances, thus alleviating the performance issues in state of the art WEAS schemes.

The main contributions of this paper are as follows: An adaptive energy detection scheme is proposed which switches between WEAS and conventional ED by adaptively controlling the weights based on a novel energy difference algorithm. A novel method to compute optimised weights dynamically is proposed based on received signal history. Mathematical formulation(s) of the decision threshold for WEAS and energy difference schemes are derived, which aims at improving accuracy in decision making. An enhanced real-time noise variance estimation technique is developed with the aid of cyclic prefix in the LDACS signals. The noise variance can be estimated effectively in real-time irrespective of primary signal being on or off. A wideband spectrum sensing scheme is developed in which the detector is able to scan multiple LDACS channels at a time. The proposed technique is integrated into a cognitive radio platform on a field-programmable gate array (FPGA) platform to quantify resource overheads.

The rest of the paper is organised as follows: Section 2 discusses related works from literature that explores spectrum sensing schemes in differnent application domains. In section 3, we explain the proposed system model used for energy detection in LDACS air-to-ground system. The detailed analysis of the proposed spectrum sensing scheme is performed in Section 4, while the real-time noise variance estimation technique is explained and analysed in Section 5. Section 6 deals with the simulation set-up and integration of the scheme onto a cognitive radio platform on an FPGA. The results of our evaluation and hardware implementation is presented in Section 7. Section 8 concludes the paper.

2 Related Works

2.1 Spectrum Sensing

Numerous spectrum sensing techniques are proposed in the literature and these techniques differ in their detection accuracies and computational complexities. The incoherent type of spectrum sensing techniques such as Energy Detection (ED) [28] and eigenvalue detection [31] does not require any prior information regarding the signals transmitted by the Primary aircraft. The coherent techniques utilise the prior knowledge about the signals (known patterns or its statistical properties such as mean and autocorrelation) for the detection. The main coherent spectrum sensing techniques are matched filter detection [21], cyclostationary feature detection [30] and other correlator based techniques. Usually, these techniques employ correlation with the known parameters of the signal for the detection that requires more computational resources. Moreover, the real-time performance of the system is affected while using these coherent techniques, as the time required for the sensing is also longer in these techniques. Eigenvalue detection compares the maximum to minimum ratio of the eigenvalue of the covariance matrix of the received sig-

nal with a predefined threshold [31]. It requires highly complex tasks such as the computation of the covariance matrix and the eigenvalue decomposition requiring intensive computations. Beyond this, the decision threshold is also a challenging task, limiting their suitability for aeronautical applications. ED-based techniques are getting important traction in this scenario due to their low complexity and incoherent nature [28]. In ED, the signal detection is done by comparing the received energy over time and frequency with a predefined threshold. However, the conventional ED suffers from many challenges such as proper estimation of noise variance, inability to distinguish LDACS signals and other malicious user signals and relatively high SNR wall for the correct decision[30].

Many spectrum sensing techniques based on alternative forms of ED have been proposed to improve the detection performance. Double threshold ED is one among them [32] and it utilises two thresholds for the decision process. Noise uncertainty problem can be reduced by double threshold ED, but it suffers from sensing round repletion problem if the received energy falls in the confusion region. In [18], an energy-difference detection based spectrum sensing technique is proposed for LDACS signals by exploiting the unique spectral shape in the range of interest after removing the DME pulses from the neighboring channels. The algorithm requires twice the computational resources as that of conventional ED as it requires the extraction of the two channels (one LDACS channel and one DME channel) and finds their energy differences. Spectrum sensing techniques for the detection of LDACS signals is hardly addressed in the literature, which is the problem addressed in our current work.

The proposed scheme improves the detection performance of the spectrum sensing schemes proposed in [14, 20] by introducing an energy difference algorithm in the WEAS with optimised weights. In [14], an Improved Energy Detection (IED) scheme is proposed. In this scheme, the vacant channels are identified by a three-step detection procedure. It utilises the received signal energy from previous $L(L \geq 2)$ sensing slots in the detection process. However, the detection performance of the IED is better than that of conventional ED when the PU is static, it has less impact when the PU changes its state frequently. In [20], a sequential energy detection method is proposed. Similar to [14], the weighted sum of a fixed number of past energy observations are considered for the decision making. The intermittent PU activity is modelled using two state Markov chain. The detection performance of this scheme also degrades during frequent PU state changes. In order to solve the performance degradation during state changes of the PU, the proposed scheme introduces an energy difference (difference of received signal energy from the current and the previous sensing slots) algorithm to adaptively control the participation of past energy observations in the decision making with adaptive weights ($w = 1$ or $0 \leq w \leq 1$).

2.2 LDACS for Air-to-Ground Communication

LDACS is a cellular communication system comprising a network of Ground Stations (GS) and airborne stations. LDACS is designed to deploy as an inlay system between two Distance Measuring Equipment (DME) channels in the frequency range 960-1164 MHz. LDACS contains a total of 46 channels with equal number of uplink and downlink channels. The uplink and downlink are separated by an

offset of 63 MHz to avoid mutual interference. Each channel in LDACS is of bandwidth 0.5 MHz and is placed at 0.5 MHz and 1 MHz from the adjacent DME and LDACS channels respectively. LDACS uses OFDM as the modulation scheme with a maximum of 50 subcarriers for transmission spaced at 9.8 KHz apart, A DC subcarrier at the 33rd position separates the two banks of 25 subcarriers each. The dynamic allocation of the LDACS channels in an opportunistic manner improves the spectral efficiency of the future aeronautical communication systems [23, 24].

2.3 Noise Variance Estimation Techniques

Most of the spectrum sensing scheme require to estimate the noise power. Any errors in the noise estimation degrades the detection performance drastically. Removal of noise uncertainty with less complex techniques is always a big challenge. Different approaches for noise variance estimation are available in the literature. Some of the recent techniques are discussed in this section. In [16], the noise power estimation was conducted assuming the noise power level is stationary for a few minutes because the thermal power changes are very slow phenomena. In this technique, Maximum likelihood estimation on noise only samples were performed with the pre-known quite periods of primary user. In [15],exploits the frequency bins corresponding to the guard bands in the area of interest. In [12], prior-knowledge of the cyclic prefix is used to estimate the noise variance. In this technique the noise variance is estimated from the received same signal samples used for detection process. The main advantage over the conventional techniques is that the noise variance can be estimated effectively, irrespective of the state of the channel (occupied/vacant). In this work, the technique proposed in [12] is enhanced to cater the cyclic prefix structure of the LDACS signal for the effective noise variance estimation.

3 System Model for Energy Detection

The spectrum sensing problem can be modeled as a binary hypothesis problem with two hypothesis $\mathcal{H}_0$ and $\mathcal{H}_1$ to represent absence and presence of the signal in the channel respectively.

$$y(n) = \begin{cases} w(n) & \mathcal{H}_0 \\ x(n) + w(n) & \mathcal{H}_1 \end{cases}, \tag{1}$$

where $x(n) = h(n)s(n)$ with $n = 1, 2, \ldots, N$. $h(n), s(n)$ and $w(n)$ represents channel gain, signal and additive white Gaussian noise(AWGN) respectively, and N is the number of signal samples used for the detection process. The hypothesis $\mathcal{H}_0$ represents the presence of noise samples only and $\mathcal{H}_1$ represents the presence of the LDACS signals with noise.

3.1 Test statistic

In ED, the energy over a time and frequency is calculated and compared with the threshold for the absence or presence of the signal. The test statistic of the

conventional ED as [14]

$$E_i(y_i) = \sum_{n=1}^{N} |y_i(n)|^2 \underset{\mathcal{H}_0}{\overset{\mathcal{H}_1}{\gtrless}} \lambda_i, \tag{2}$$

where $E_i(y_i)$ is the test statistic and λ_i is the threshold for the i^{th} sensing slot. The detector selects the hypothesis with the comparison of the threshold λ_i. The distribution of the test statistic under $\mathcal{H}_0$, using central limit theorem (CLT) is given as [4, 12, 14, 22]

$$E_i \sim \mathcal{N}(N\sigma_{w_i}^2, 2N\sigma_{w_i}^4), \qquad \mathcal{H}_0, \tag{3}$$

where $\mathcal{N}(\mu, \sigma^2)$ stands for Gaussian distribution with mean μ and variance σ^2.

The distribution of the PU signals (LDACS signals) is not known perfectly. The distribution of test statistic under $\mathcal{H}_1$ assuming gaussian distribution using CLT is given as [4, 12, 14, 22],

$$E_i \sim \mathcal{N}\Big(N\big(\sigma_{x_i}^2 + \sigma_{w_i}^2\big), 2N\big(\sigma_{x_i}^2 + \sigma_{w_i}^2\big)^2\Big) \qquad \mathcal{H}_1. \tag{4}$$

The probability of false alarm (P_{fa}) and the probability detection(P_d) for the conventional ED can be obtained from (3) and (4) respectively and is given in (5) and (6) respectively as [14],

$$P_{fa} = P(E_i > \lambda_i/\mathcal{H}_0) = Q\left(\frac{\lambda_i - N\sigma_{w_i}^2}{\sqrt{2N\sigma_{w_i}^4}}\right), \tag{5}$$

$$P_d = P(E_i > \lambda_i/\mathcal{H}_1) = Q\left(\frac{\lambda_i - N(\sigma_{x_i}^2 + \sigma_{w_i}^2)}{\sqrt{2N\big(\sigma_{x_i}^2 + \sigma_{w_i}^2\big)^2}}\right), \tag{6}$$

where $Q(.)$ is Q-function and λ_i is the decision threshold. From (5), decision threshold for a particular false alarm rate is given as [14]

$$\lambda_i = \Big(Q^{-1}(P_{fa})\sqrt{2N} + N\Big)\sigma_{w_i}^2. \tag{7}$$

The conventional energy detection suffers various challenges such as noise uncertainty(NU), relatively high SNR wall [5, 17] for desired detection accuracy compared to feature detection techniques and inability to distinguish the malicious users. The decision accuracy can be improved if the two hypotheses are separated effectively. To address this challenge, the variance of the test statistic (received energy E_i for the conventional ED) needs to be minimised. In this work, we have modified the sequential energy detection schemes in [14, 20] by introducing an energy difference algorithm to detect the PU state changes. Proper mathematical formulations are derived for the weighted averaging and for the energy difference detection schemes.

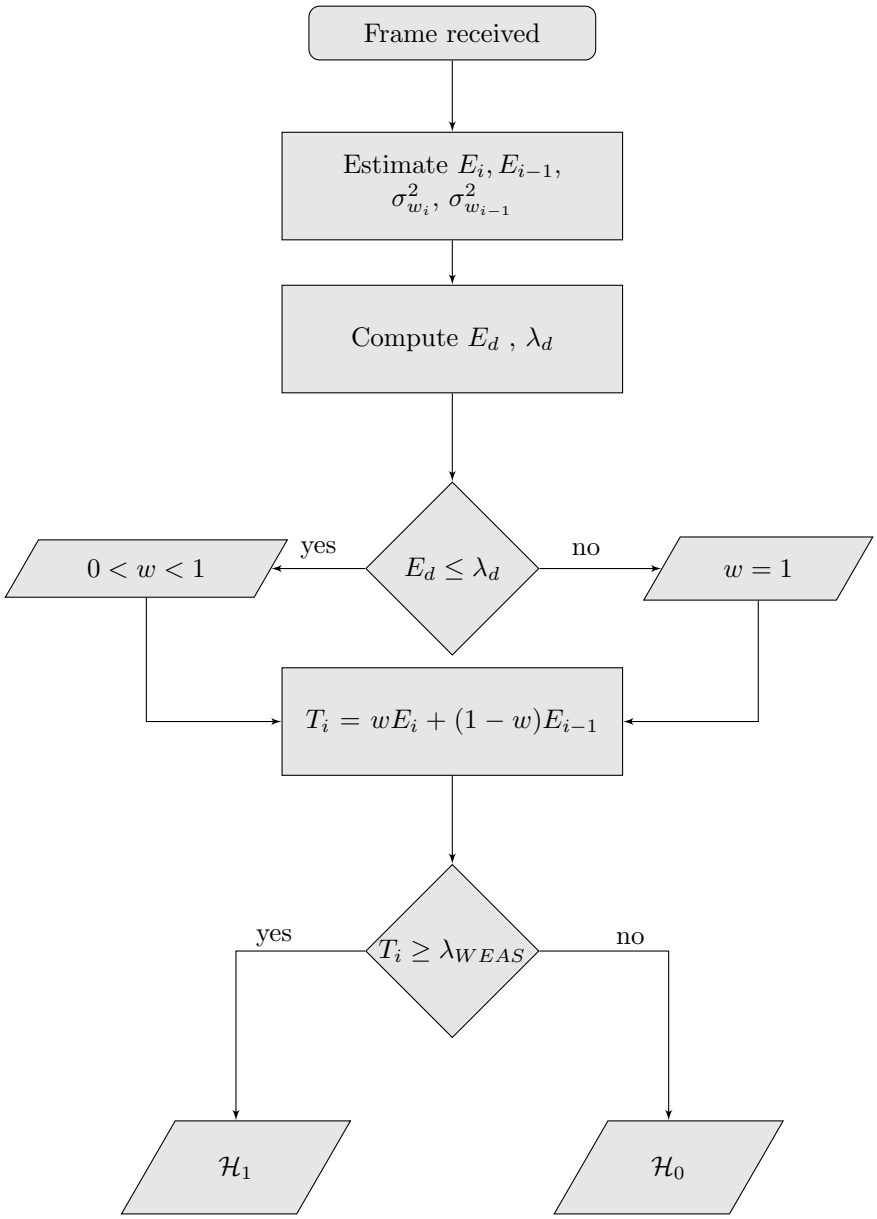

Fig. 1 Flowchart of the energy difference incorporated weighted energy averaging scheme.

4 Proposed Spectrum Sensing Scheme

The performance metric in energy detection can be improved by reducing the effective variance of the test statistic. In this work, the correlation between the current and past energy measurements is exploited for lowering the SNR wall to achieve the desired detection accuracy. The flow chart for the proposed scheme

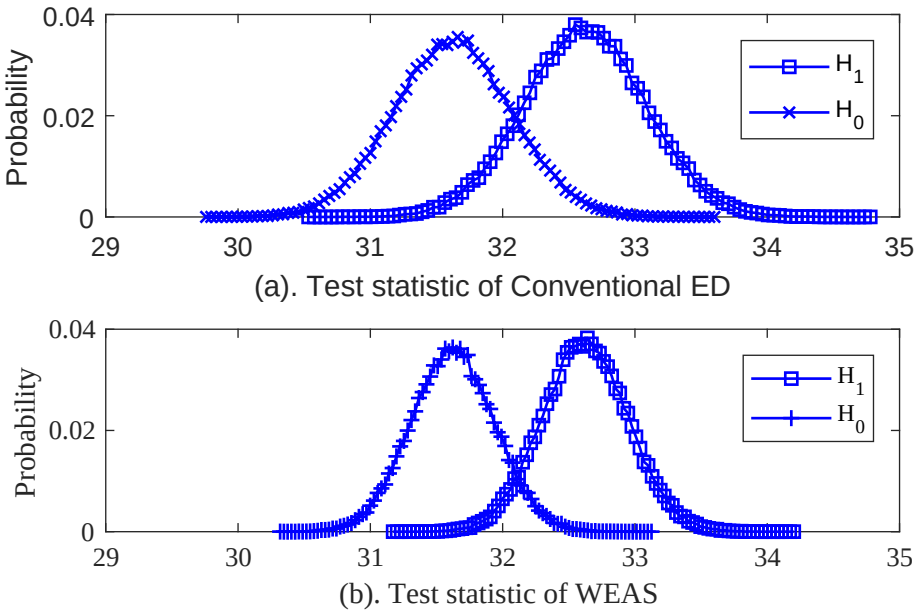

Fig. 2 The probability distribution for the test statistic. (a) Conventional ED (b) WEAS.

is given in Fig. 1. The scheme works as follows; primarily, the energy difference between the current and previous sensing slots ($E_d = E_i - E_{i-1}$) is calculated. This energy difference is compared with a pre-specified threshold (The details of threshold calculation is given in Section 4.4). This energy difference algorithm is used to identify the sudden rise or drop of the received energy in the consecutive sensing intervals. A state change(either $\mathcal{H}_0 \rightarrow \mathcal{H}_1$ or $\mathcal{H}_1 \rightarrow \mathcal{H}_0$) is indicated if $|E_d| > \lambda_d$. In that case, only the received energy from the current sensing slot is considered for decision making ($w = 1$). On the other side, when the PU is identified as static (either $\mathcal{H}_0 \rightarrow \mathcal{H}_0$ or $\mathcal{H}_1 \rightarrow \mathcal{H}_1$), the weighted sum of the received energy ($0 \leq w \leq 1$) from the current and previous time slots is considered for the decision making. This adaptive switching is controlled by adaptively applying the weights for current and previous sensing slots ($0 \leq w \leq 1$). The weight w is optimized to reduce the false alarm rate by giving higher priority to the sensing interval whose noise variance is less. The details of the weight optimization are explained in Section 4.3.

Incorporating the past energy observations into the decision making improves the detection performance in static PU, as it reduces the variance of the test statistics. The probability distribution plots for the test statistic for this weighted energy averaging scheme (WEAS) and the conventional ED is shown in Fig. 2. The simulations have been carried out with 10000 signal samples at $SNR = -10$ dB. The results from the 10000 iterations are summarised in the probability distribution curves. It is clearly visible from the Fig. 2 that the common area shared by $\mathcal{H}_0$ and $\mathcal{H}_1$ (ie, the probability of error) is less for WEAS when compared to conventional ED. On the other hand, WEAS lead to performance degradation

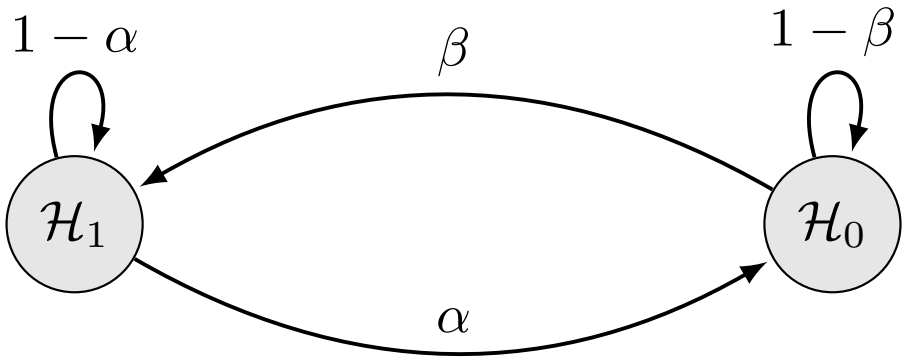

Fig. 3 The channel state change model using two state Markov chain [10].

during frequent state changes. To address this, we employ an energy difference algorithm to detect the state changes. The proposed algorithm adaptively controls the weights of the current and past energy observation in the calculation of the test statistic thereby adaptively switch between the WEAS and conventional ED depends upon the static and frequent state change conditions respectively.

4.1 The channel state model

Different approaches [6, 19, 20, 29] are available in the literature to model the intermittent PU activity in cognitive radio. In this work, two state Markov chain [10] model is adopted to create a practical scenario. Let α be the probability that the channel changes it state from busy ($\mathcal{H}_1$) to idle ($\mathcal{H}_0$) and β be the probability that the channel changes its state from idle to busy. The channel state change is modeled as a two state Markov chain and is shown in Fig. 3. The values of α and β can be expressed as a function of the state probabilities $P(\mathcal{H}_1)$ and $P(\mathcal{H}_0)$ of the channel with the aid of Markov model. The values of $P(B)$ and $P(I)$ are obtained from the historical data.

$$P(\mathcal{H}_1) = (1-\alpha)P(\mathcal{H}_1) + \beta P(\mathcal{H}_0) \tag{8}$$

$$P(\mathcal{H}_0) = \alpha P(\mathcal{H}_1) + (1-\beta)P(\mathcal{H}_0) \tag{9}$$

$$P(\mathcal{H}_1) = \frac{\beta}{\alpha+\beta} \tag{10}$$

$$P(\mathcal{H}_0) = \frac{\alpha}{\alpha+\beta} \tag{11}$$

4.2 Weighted Energy Averaging Scheme (WEAS)

The proposed spectrum sensing scheme considers the received energy of the previous time slots along with the current energy values. The test statistic T_i for the

WEAS is defined in (12).

$$T_i = wE_i + (1-w)E_{i-1} \tag{12}$$

where E_i and (E_{i-1}) are the received signal energy from the current sensing slot and previous sensing slot respectively.

As mentioned, a two-state Markov chain is used to represent the state transitions. As shown in Fig. 3, there are four possibilities of state transitions in the WEAS ($\mathcal{H}_0 \rightarrow \mathcal{H}_0, \mathcal{H}_0 \rightarrow \mathcal{H}_1, \mathcal{H}_1 \rightarrow \mathcal{H}_0$ and $\mathcal{H}_1 \rightarrow \mathcal{H}_1$). The distribution of the test statistic of WEAS for all possible state transitions are derived using (3) and (4) and is given in (13).

$$T_i \sim \begin{cases} \mathcal{N}\Bigg(N\Big(w\sigma^2_{w_i} + (1-w)\sigma^2_{w_{i-1}}\Big), \\ 2N\Big(w^2\sigma^4_{w_i} + (1-w)^2\sigma^4_{w_{i-1}}\Big)\Bigg) & \mathcal{H}_0 \rightarrow \mathcal{H}_0 \\ \mathcal{N}\Bigg(N\Big(w\big(\sigma^2_{w_i} + \sigma^2_{x_i}\big) + (1-w)\sigma^2_{w_{i-1}}\Big), \\ 2N\big(w^2\big(\sigma^2_{w_i} + \sigma^2_{x_i}\big)^2 + (1-w)^2\sigma^4_{w_{i-1}}\big)\Bigg), & \mathcal{H}_0 \rightarrow \mathcal{H}_1 \\ \mathcal{N}\Bigg(N\Big(w\sigma^2_{w_i} + (1-w)\big(\sigma^2_{w_{i-1}} + \sigma^2_{x_{i-1}}\big)\Big), \\ 2N\big(w^2\sigma^4_{w_i} + (1-w)^2\big(\sigma^2_{w_{i-1}} + \sigma^2_{x_{i-1}}\big)^2\big)\Bigg), & \mathcal{H}_1 \rightarrow \mathcal{H}_0 \\ \mathcal{N}\Bigg(N\Big(w\big(\sigma^2_{w_i} + \sigma^2_{x_i}\big) + (1-w)\big(\sigma^2_{w_{i-1}} + \sigma^2_{x_{i-1}}\big)\Big), \\ 2N\big(w^2\big(\sigma^2_{w_i} + \sigma^2_{x_i}\big)^2 + (1-w)^2\big(\sigma^2_{w_{i-1}} + \sigma^2_{x_{i-1}}\big)^2\big)\Bigg), & \mathcal{H}_1 \rightarrow \mathcal{H}_1 \end{cases} \tag{13}$$

The first term of (13) indicates the distribution of the test statistic when the PU is idle for both i^{th} and $i-1^{th}$ sensing intervals ($\mathcal{H}_0 \rightarrow \mathcal{H}_0$). The second term corresponds to a state change from idle to busy($\mathcal{H}_0 \rightarrow \mathcal{H}_1$), third term is used to represent the state change from busy to idle ($\mathcal{H}_1 \rightarrow \mathcal{H}_0$) and the last term is the distribution of the test statistic when the PU is busy on both the sensing intervals($\mathcal{H}_1 \rightarrow \mathcal{H}_1$). The average probability of false alarm and the probability of detection can be derived from (13).

4.2.1 Probability of false alarm

The average probability of false alarm has been derived from the first and third terms of (13). During $\mathcal{H}_0 \rightarrow \mathcal{H}_0$, the probability of false alarm P_{fa} is,

$$\begin{aligned} P_{fa}(WEAS/\mathcal{H}_0 \rightarrow \mathcal{H}_0) &= P\Big(T_i > \lambda_{WEAS}/(\mathcal{H}_0 \rightarrow \mathcal{H}_0)\Big) \\ &= Q\left(\frac{\lambda_{WEAS} - N\big(w\sigma^2_{w_i} + (1-w)\sigma^2_{w_{i-1}}\big)}{\sqrt{2N\big(w^2\sigma^4_{w_i} + (1-w)^2\sigma^4_{w_{i-1}}\big)}}\right) \end{aligned} \tag{14}$$

Similarly for $\mathcal{H}_1 \rightarrow \mathcal{H}_0$, the probabilty of false alarm, P_{fa} is obtained from third term of (13),

$$\begin{aligned} P_{fa}(WEAS/\mathcal{H}_1 \rightarrow \mathcal{H}_0) &= P\Big(T_i > \lambda_{WEAS}/(\mathcal{H}_1 \rightarrow \mathcal{H}_0)\Big) \\ &= Q\left(\frac{\lambda_{WEAS} - N\Big(w\sigma_{w_i}^2 + (1-w)\big(\sigma_{w_{i-1}}^2 + \sigma_{x_{i-1}}^2\big)\Big)}{\sqrt{2N\big(w^2\sigma_{w_i}^4 + (1-w)^2\big(\sigma_{w_{i-1}}^2 + \sigma_{x_{i-1}}^2\big)^2\big)}}\right) \end{aligned} \tag{15}$$

The average probability of false alarm of the WEAS is given as,

$$\begin{aligned} P_{fa}(WEAS) = (1-\beta)P\Big(T_i > \lambda_{WEAS}/(\mathcal{H}_0 \rightarrow \mathcal{H}_0)\Big) \\ +\alpha P\Big(T_i > \lambda_{WEAS}/(\mathcal{H}_1 \rightarrow \mathcal{H}_0)\Big) \end{aligned} \tag{16}$$

where $1-\beta$ is the probability of the transition $\mathcal{H}_0 \rightarrow \mathcal{H}_0$ and α is the probability of the transition $\mathcal{H}_1 \rightarrow \mathcal{H}_0$ as shown in Fig. 3.

4.2.2 Probability of detection

The average probability of detection has been derived from the second and fourth terms of (13). During $\mathcal{H}_0 \rightarrow \mathcal{H}_1$, the probability of detection is obtained from second term of (13),

$$\begin{aligned} P_d(WEAS/\mathcal{H}_0 \rightarrow \mathcal{H}_1) &= P\Big(T_i > \lambda_{WEAS}/(\mathcal{H}_0 \rightarrow \mathcal{H}_1)\Big) \\ &= Q\left(\frac{\lambda_{WEAS} - N\Big(w\big(\sigma_{w_i}^2 + \sigma_{x_i}^2\big) + (1-w)\sigma_{w_{i-1}}^2\Big)}{\sqrt{2N\Big(w^2\big(\sigma_{w_i}^2 + \sigma_{x_i}^2\big)^2 + (1-w)^2\sigma_{w_{i-1}}^4\Big)}}\right) \end{aligned} \tag{17}$$

Similarly, for $\mathcal{H}_1 \rightarrow \mathcal{H}_1$, the probability of detection obtained from fourth term of (13) and is given in (18).

$$\begin{aligned} P_d(WEAS/\mathcal{H}_1 \rightarrow \mathcal{H}_1) &= P\Big(T_i > \lambda_{WEAS}/(\mathcal{H}_1 \rightarrow \mathcal{H}_1)\Big) \\ &= Q\left(\frac{\lambda_{WEAS} - N\Big(w\big(\sigma_{w_i}^2 + \sigma_{x_i}^2\big) + (1-w)\big(\sigma_{w_{i-1}}^2 + \sigma_{x_{i-1}}^2\big)\Big)}{\sqrt{2N\big(w^2\big(\sigma_{w_i}^2 + \sigma_{x_i}^2\big)^2 + (1-w)^2\big(\sigma_{w_{i-1}}^2 + \sigma_{x_{i-1}}^2\big)^2\big)}}\right) \end{aligned} \tag{18}$$

The average probability of detection of the WEAS is given as,

$$\begin{aligned} P_d(WEAS) = \beta P\Big(T_i > \lambda_{WEAS}/(\mathcal{H}_0 \rightarrow \mathcal{H}_1)\Big) \\ +(1-\alpha)P\Big(T_i > \lambda_{WEAS}/(\mathcal{H}_1 \rightarrow \mathcal{H}_1)\Big) \end{aligned} \tag{19}$$

4.2.3 The decision threshold

The decision threshold λ_{WEAS} for the WEAS is calculated from (14) for a fixed false alarm rate and assuming no state change.

$$\lambda_{WEAS} = \sqrt{2N\big(w^2\sigma^4_{w_i} + (1-w)^2\sigma^4_{w_{i-1}}\big)}Q^{-1}(P_{fa}) + N\big(w\sigma^2_{w_i} + (1-w)\sigma^2_{w_{i-1}}\big) \tag{20}$$

When $\sigma^2_{w_i} = \sigma^2_{w_{i-1}}$, $\lambda_{WEAS} = \lambda_{avg}$ and is given in (21).

$$\lambda_avg = \Big(Q^{-1}\big(P_{fa}\big)\sqrt{N} + N\Big)\sigma^2_{w_i} \tag{21}$$

When the PU state changes (either $\mathcal{H}_0 \rightarrow \mathcal{H}_1$ or $\mathcal{H}_1 \rightarrow \mathcal{H}_0$), the detection schemes proposed in [14] and [20] degrade its performance (refer (15) and (17)). The state changes of the PU are not considered in these schemes. In proposed energy detection scheme, an energy difference algorithm is used to find the state changes. The energy-difference $|E_D|(E_D = E_i - E_{i-1})$is compared with predefined threshold λ_d to find the state change. As explained in the flow chart of the proposed scheme, when state change happens, decision will be made using received energy of the current slot only$(ie, w = 1, \lambda_{WEAS} = \lambda_i$ and $T_i = E_i$).

4.3 Weight Optimization

The weight optimization is required when there is no state change ($\mathcal{H}_0 \rightarrow \mathcal{H}_0$ and $\mathcal{H}_1 \rightarrow \mathcal{H}_1$). In this work, the weight optimization is carried out on the basis of $\mathcal{H}_0 \rightarrow \mathcal{H}_0$ as it requires knowledge about noise variance only. To do this, the first term of (13), $\mathcal{N}\Big(N\big(w\sigma^2_{w_i} + (1-w)\sigma^2_{w_{i-1}}\big), 2N\Big(w^2\sigma^4_{w_i} + (1-w)^2\sigma^4_{w_{i-1}}\Big)\Big)$ is considered. The variance in the above distribution needs to be minimised to reduce the effective false alarm rate. The optimal value of w by minimizing $2N\Big(w^2\sigma^4_{w_i} + (1-w)^2\sigma^4_{w_{i-1}}\Big)$ and is obtained by,

$$\frac{\partial}{\partial w}2N\Big(w^2\sigma^4_{w_i} + (1-w)^2\sigma^4_{w_{i-1}}\Big) = 0 \tag{22}$$

The optimal value of w obtained from (22) is,

$$w = \frac{\sigma^4_{w_{i-1}}}{\sigma^4_{w_i} + \sigma^4_{w_{i-1}}} \tag{23}$$

From (23) it is clear that more weight is given to the time slot having less noise variance that results in better decision accuracy. For$\sigma^2_{w_i} = \sigma^2_{w_{i-1}}$, the optimal weight is 0.5, and is observed in the simulation results too.

4.4 Energy-Difference Algorithm

The state change can be detected with the energy-difference algorithm. The difference of the received energy for the current and previous time slots ($E_d = E_i - E_{i-1}$) is compared with the predefined thresholds for the state change detection. The distribution of the test statistic of the energy-difference for different state changes is derived from (3) and (4) and is given in (24).

$$E_{Di} \sim \begin{cases} \mathcal{N}\Big(N\Big(\sigma^2_{w_i} - \sigma^2_{w_{i-1}}\Big), \\ 2N\Big(\sigma^4_{w_i} + \sigma^4_{w_{i-1}}\Big)\Big), & \mathcal{H}_0 \to \mathcal{H}_0 \\ \mathcal{N}\Big(N\Big(\big(\sigma^2_{w_i} + \sigma^2_{x_i}\big) - \sigma^2_{w_{i-1}}\Big), \\ 2N\big(\big(\sigma^2_{w_i} + \sigma^2_{x_i}\big)^2 + \sigma^4_{w_{i-1}}\big)\Big), & \mathcal{H}_0 \to \mathcal{H}_1 \\ \mathcal{N}\Big(N\Big(\sigma^2_{w_i} - \big(\sigma^2_{w_{i-1}} + \sigma^2_{x_{i-1}}\big)\Big), \\ 2N\big(\sigma^4_{w_i} + \big(\sigma^2_{w_{i-1}} + \sigma^2_{x_{i-1}}\big)^2\big)\Big), & \mathcal{H}_1 \to \mathcal{H}_0 \\ \mathcal{N}\Big(N\Big(\big(\sigma^2_{w_i} + \sigma^2_{x_i}\big) - \big(\sigma^2_{w_{i-1}} + \sigma^2_{x_{i-1}}\big)\Big), \\ 2N\big(\big(\sigma^2_{w_i} + \sigma^2_{x_i}\big)^2 + \big(\sigma^2_{w_{i-1}} + \sigma^2_{x_{i-1}}\big)^2\big)\Big), & \mathcal{H}_1 \to \mathcal{H}_1 \end{cases} \tag{24}$$

From the distribution, the mean of the energy-difference can be defined as $\mu_d = N(\sigma^2_{w_i} - \sigma^2_{w_{i-1}})$ and $\sigma^2_d = 2N\big(\sigma^4_{w_i} + \sigma^4_{w_{i-1}}\big)$ during static channel conditions (No state changes) assuming signal power remains unchanged during the consecutive sensing durations. The differential threshold λ_d is derived from (24) and is given in (25).

$$\lambda_d = \sqrt{2N\big(\sigma^4_{w_i} + \sigma^4_{w_{i-1}}\big)}\,Q^{-1}(P_{fa}) + N\big(\sigma^2_{w_i} - \sigma^2_{w_{i-1}}\big) \tag{25}$$

Note that no state change happens if the absolute value of energy-difference is less than λ_d. The proposed spectrum sensing scheme uses an energy-difference algorithm and the weighted energy averaging scheme (WEAS) as explained in the flowchart in Fig. 1 and section 4.

5 Noise Variance Estimation

The decision thresholds in the ED based systems are highly dependent on the noise level. The detection performance degrades drastically even with minor errors in the noise variance estimation. In this scheme, we use an unbiased noise variance estimator, which exploits the pre-knowledge of cyclic prefix in the LDACS signal. Fig. 4 shows the LDACS signal frame structure. As shown in the figure, the insertion of CP induces an autocorrelation property. This property is utilized for the

consistent estimation of noise variance, irrespective of the state of the channel and the presence of primary user signal.

Let the total number of signal samples, $N = K(N_{CP}+N_D)$, where K represents the total number of OFDM symbols used for the sensing, N_{CP} is the cyclic prefix length in samples per symbol and N_D is the data length of OFDM symbol. Let define two terms E_y and ρ_y as,

$$E_y = \frac{1}{K(N_{CP}+N_D)} \sum_{n=1}^{K(N_{CP}+N_D)} |y_i(n)|^2 \tag{26}$$

$$\rho_y = \frac{1}{KN_{CP}} \sum_{n=1}^{K(N_{CP}+N_D)} \mathcal{R}\big[y_i(n)y_i(n+N_D)\big] \tag{27}$$

where $\mathcal{R}[.]$ represents the real part of the term. E_y represents the energy estimate and ρ_y is the autocorrelation strength of the received signal samples. The distribution of E_y and ρ_y are given in (28) and (29) respectively.

$$E_y \sim \begin{cases} \mathcal{N}\big(\sigma^2_{w_i}, \frac{2\sigma^4_{w_i}}{K(N_{CP}+N_D)}\big), & \mathcal{H}_0 \\ \mathcal{N}\Big((\sigma^2_{x_i}+\sigma^2_{w_i}), \frac{2\left(\sigma^2_{x_i}+\sigma^2_{w_i}\right)^2}{K(N_{CP}+N_D)}\Big), & \mathcal{H}_1 \end{cases} \tag{28}$$

$$\rho_y \sim \begin{cases} \mathcal{N}\big(0, \frac{\sigma^4_{w_i}(N_{CP}+N_D)}{2KN^2_{CP}}\big), & \mathcal{H}_0 \\ \mathcal{N}\Big(\sigma^2_{x_i}, \frac{\left(\sigma^2_{x_i}+\sigma^2_{w_i}\right)^2(N_{CP}+N_D)+\sigma^4_x N_{CP}}{2KN^2_{CP}}\Big), & \mathcal{H}_1 \end{cases} \tag{29}$$

The unbiased estimate of noise variance is defined using E_x and ρ_x as,

$$\hat{\sigma}^2_{w_i} = E_y - \rho_y \tag{30}$$

From (28) and (29), the distribution of $\hat{\sigma}^2_{w_i}$ is derived and is given in (31).

$$\hat{\sigma}^2_{w_i} \sim \begin{cases} \mathcal{N}\Big(\sigma^2_{w_i}, \frac{2\sigma^4_{w_i}}{K(N_{CP}+N_D)} \\ \quad + \frac{\sigma^4_{w_i}(N_{CP}+N_D)}{2KN^2_{CP}}\Big) & \mathcal{H}_0 \\ \mathcal{N}\Big(\sigma^2_{w_i}, \frac{2\left(\sigma^2_{x_i}+\sigma^2_{w_i}\right)^2}{K(N_{CP}+N_D)} \\ \quad + \frac{\left(\sigma^2_{x_i}+\sigma^2_{w_i}\right)^2(N_{CP}+N_D)+\sigma^4_x N_{CP}}{2KN^2_{CP}}\Big) & \mathcal{H}_1 \end{cases} \tag{31}$$

It can be observed from (31) that the variance of $\hat{\sigma}^2_{w_i}$ asymptotically turns to zero. Hence, the consistency and unbiased nature of the proposed noise variance

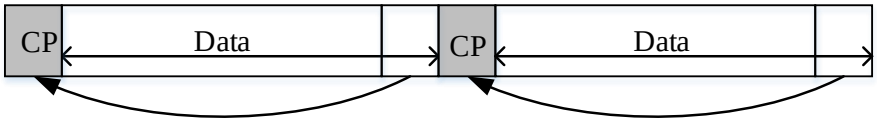

Fig. 4 Time domain frame structure of OFDM based LDACS signals.

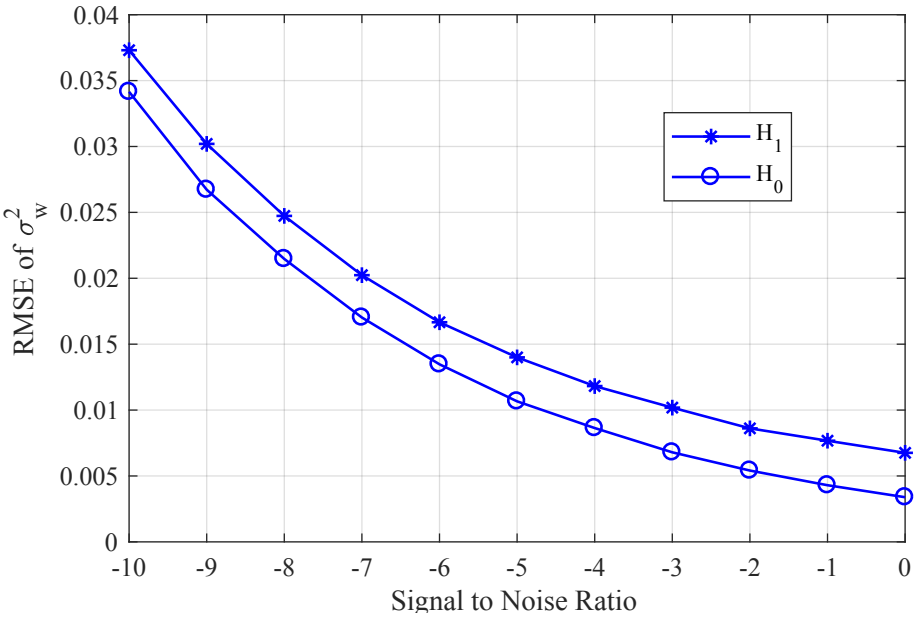

Fig. 5 RMSE of estimated noise power versus SNR.

technique is proved. The root mean square error (RMSE) of the estimated noise power is plotted in Fig. 5 for both the hypotheses. RMSE is relatively higher when the PU signal is present because the variance of $\hat{\sigma}^2_{w_i}/\mathcal{H}_1$ is high compared to $\hat{\sigma}^2_{w_i}/\mathcal{H}_0$ (refer (31)).

6 Simulation Set-up and FPGA Implementation

6.1 Simulation Set-up

6.1.1 LDACS signal generation

A wideband spectrum sensing scheme is developed to scan multiple LDACS spectral holes from a range of frequencies. For the simulation study,we consider the sampling frequency of 4 MHz and that enables to scan any LDACS channel within this 4 MHz range(Include 4 LDACS and 4 DME channels each having a bandwidth of 0.5 MHz). To imitate the real-world scenario, we have generated the LDACS baseband signals according to the specifications given in [23], and the Matlab code for the same is provided by DLR (German space agency) [2]. The parameters used to simulate LDACS signals are given in Table 1.

6.1.2 Filter architecture

A digital filter bank is used to split the wide band into several sub-bands. In this work, the fast filter bank (FFB) based channeliser proposed in [8, 13], used for

Table 1 Simulation Parameters for LDACS Signal Generation

Parameter	Value
FFT size	64
Sampling time	1.6 μs
Sub-carrier spacing	9.765625 KHz
Cyclic prefix ratio	11/64
Used subcarriers	50
Lower frequency guard sub-carriers	7
Higher frequency guard sub-carriers	6

obtaining uniform sub-bands meeting the stringent LDACS spectral mask specifications with low complexity. An 8-channel FFB design is used in the spectrum sensing unit. Out of these 8 channels, 4 alternative channels used to scan LDACS channels.

6.2 FPGA Implementation

To evaluate the resource overheads, we implement the proposed spectrum sensing scheme and integrate it into the baseband of our cognitive radio platform on the Xilinx Zynq ZC706 board [25]. Fig. 6a shows the integration of the spectrum sensing scheme into the receive path of our radio platform. As shown in the figure, to enable the strong coupling between the software and hardware, an ARM processor, and a Programmable Logic (PL) are integrated into the Zynq architecture. Channelization, spectrum sensing, and the RF interfaces are implemented in the PL region of Zynq. The PL has dedicated interfaces to communicate with software functionalities running on the ARM core. Dedicated memory access (DMA) enables high-speed interfaces between the baseband modules and software. The parametric and the partial reconfiguration techniques initiated through simple software APIs offers high-speed dynamic adaptability.

The higher level architecture of the sensing scheme is shown in Fig. 6b. The implementation strategy is to minimise the resource consumption by using building boxes that gets reused within the respective computational stages using a hierarchical state-machine. These building boxes are built around the DSP block primitive to compute complex multiplication, multiply-accumulate and division operations that are required in the estimation. We use 16-bit fixed-point representation for inputs and 32-bit fixed point representation for intermediate steps, with rounding to fit wider intermediate results back to 32-bits. The received information from the antenna is post-processed (RF domain) and fed into the channeliser that provides 4 alternative LDACS channels which are fed into the receive path buffers. One of the channels is chosen at a time for spectrum sensing and is fed into an autocorrelation logic which computes the energy of the received signal over 10000 samples (E, σ_w^2). The autocorrelation logic is a shift-register delay chain of 64-elements, while complex multiplications at the tap outputs are mapped onto DSP blocks. Further, the state machine (marked SM) initiates the computation

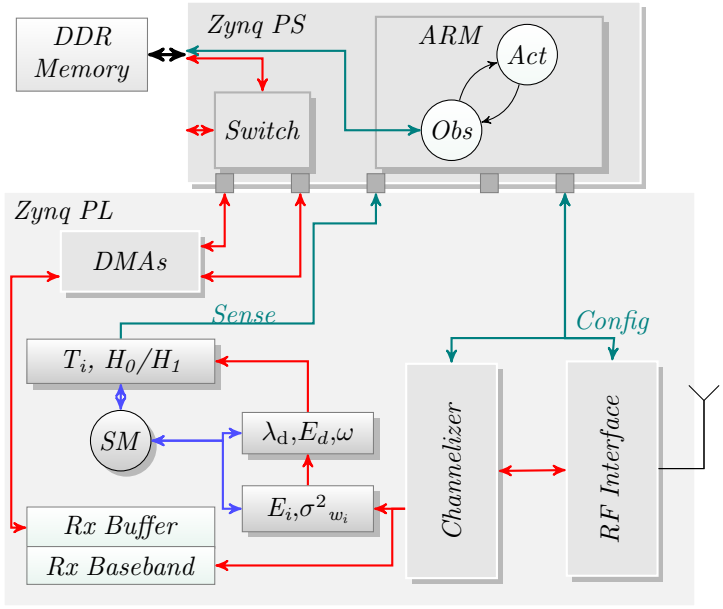

(a)

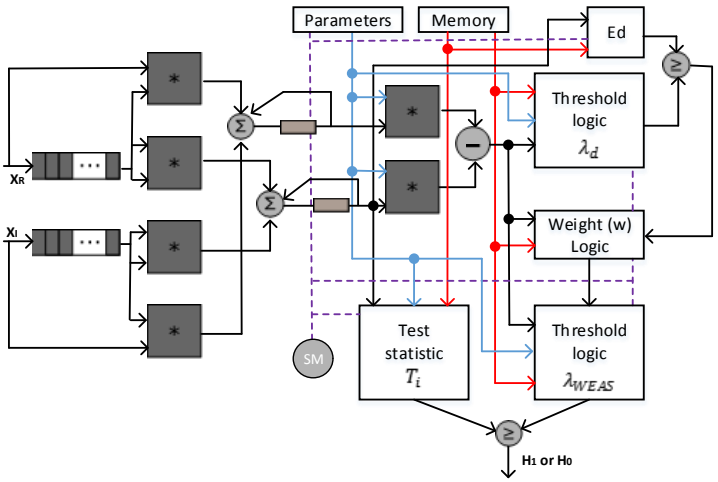

(b)

Fig. 6 Higher level architecture of the proposed system (a). Integration of spectrum sensing logic into the receive path of the LDACS radio platform. (b). Hardware architecture of the proposed sensing scheme.

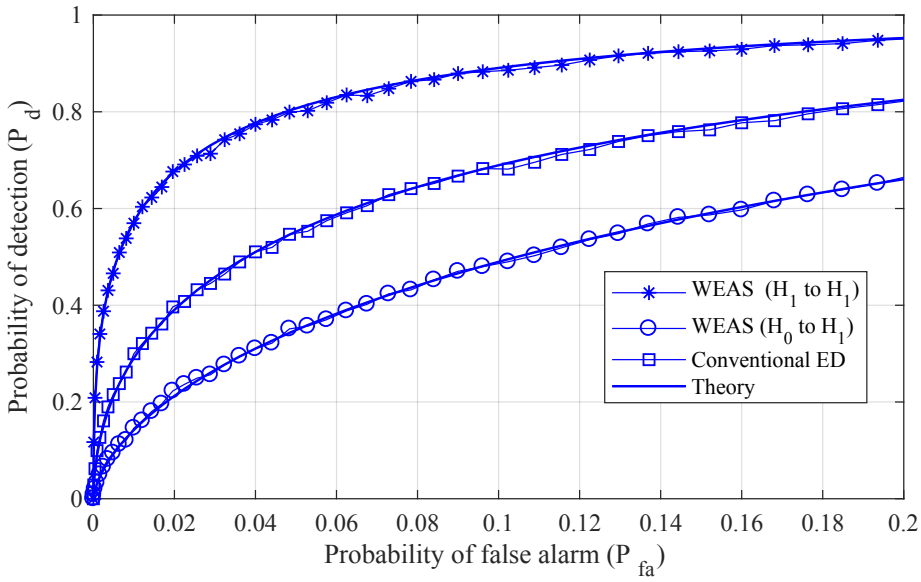

Fig. 7 Detection performance of sequential ED: Probability of detection during Static channel ($\mathcal{H}_1 \rightarrow \mathcal{H}_1$) and during state change conditions ($\mathcal{H}_0 \rightarrow \mathcal{H}_1$)(at SNR=-16 dB).

of differential threshold λ_d and the energy difference E_d. Based on the results of the energy difference algorithm, the SM initiates the weight optimization process. Once done, the SM switches to compute the test statistic and the decision threshold based on the energies (E_i and E_{i-1}), weight w, and the noise variances(σ_{w_i} and $\sigma_{w_{i-1}}$) determine if the channel is vacant or in use. The information is passed to the cognitive logic in ARM cores which can initiate a transmission in the vacant channel or configure the hardware switch to evaluate other channels. The computed parameters are stored in dedicated per-channel registers in the hardware for use in subsequent scan intervals. The state machine transitions are controlled by the parameters like the number of samples to be observed, window the depth and so on, which are configured into the parameter memory. Thus the logic can perform detection by observing a larger number of samples to boost the detection accuracy at low SNR values by altering the register value(s).

7 Results and Discussions

The performance of the proposed scheme is analysed using simulation studies. The LDACS signals are generated according to the specifications and the detection performance is evaluated for different noise levels. The performances are evaluated for static PU and frequent state change conditions and the average detection performance also evaluated. The signal energy and the noise variance are estimated from 10000 signal samples and the detection performance is average out from 10000 iterations. The state change probabilities α and β are set to 0.001 and 0.1 for static PU and frequent state change conditions respectively [20].

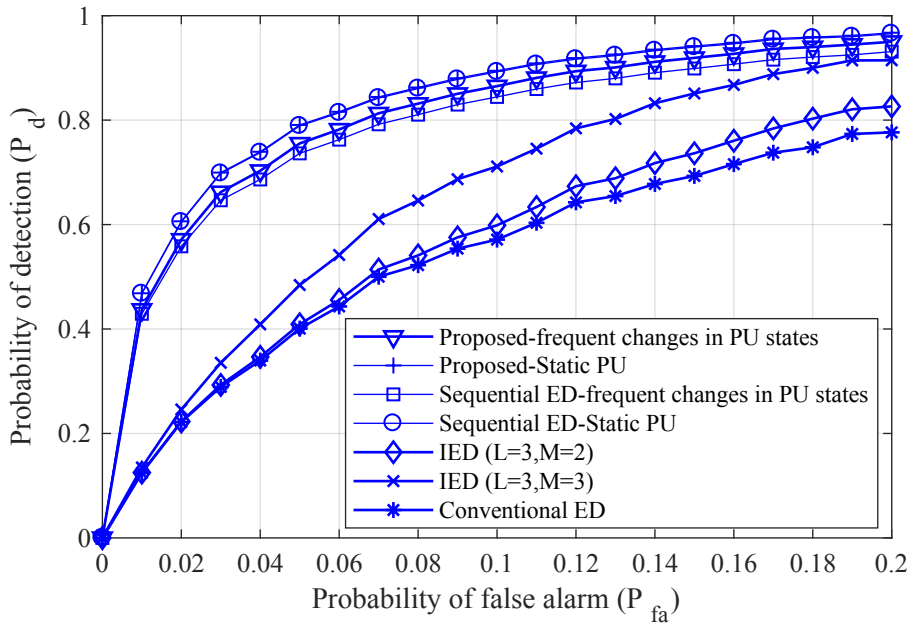

Fig. 8 Average detection performance comparison of the Conventional ED, IED [14], sequential ED [20] and the energy difference incorporated WEAS (proposed scheme) in static PU and frequent PU state cases.

The detection performances of WEAS with static PU and frequent state change conditions and the conventional ED are compared in Fig. 7. The receiver operating characteristic (ROC) curves are plotted for an SNR=-16dB. Results show that the WEAS without considering the state changes [20] under-performs when a state change occurs ($\mathcal{H}_0 \rightarrow \mathcal{H}_1$ here). At the same time, providing noticeably better performance for the static channel conditions. The proposed scheme intended to take this advantage during static channel conditions and not to lose the performance when there is a state change. The average detection performance of the proposed scheme is uplifted with the adaptive choice of the sensing scheme.

The average detection performance of the proposed scheme, conventional ED, IED [14], and the sequential ED [20] are compared in Fig. 8. For IED scheme, the parameters L and M set to 3 for imitating the static PU and M=2 for representing a state change. L corresponds to the total number of sensing information considered for averaging and M corresponds to the number of sensing intervals where PU is actually present. The parameters α and β are set to 0.001 and 0.1 for static PU and frequent state change conditions respectively for the sequential ED [20] and the prosed scheme. Results indicate that regular WEAS and the proposed scheme provides identical performance during static channel conditions. On the other hand, During frequent state change scenarios, the detection performance of the proposed scheme is better than that of sequential ED, IED and the conventional ED schemes. Here, the sequential ED also provides comparable performance during static channel conditions because of the optimised weights used

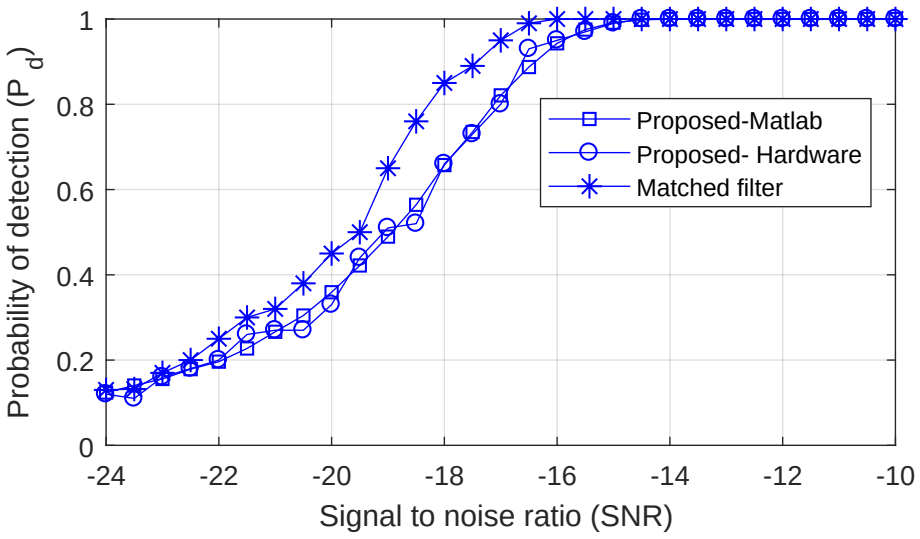

Fig. 9 Detection performance comparison of the proposed technique (Matlab and hardware results) and Matched filtering based sensing [26].

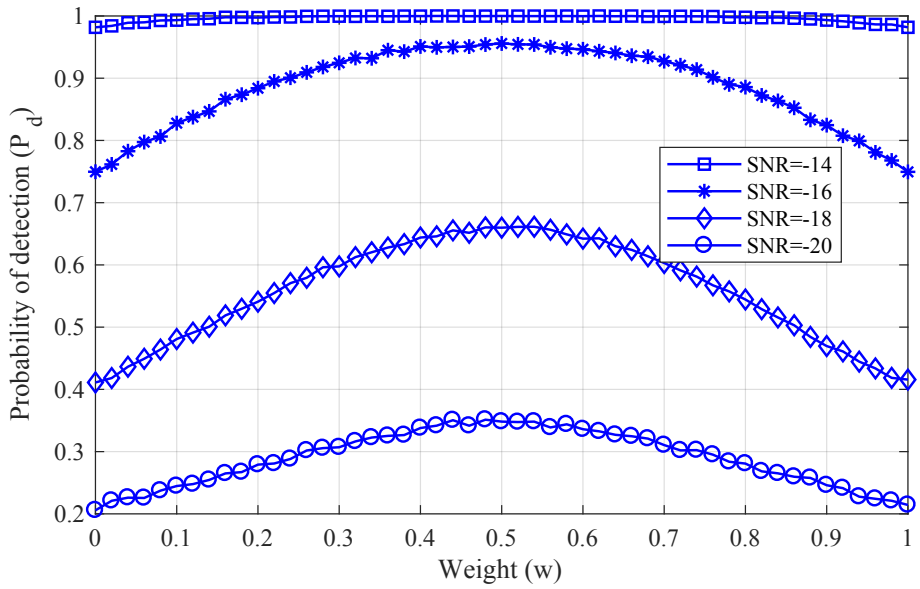

Fig. 10 Effect of weight in WEAS for different signal to noise ratios (SNR's).

for the computation of test statistic. In [20], the authors just averaged out the energies not considering the optimal weights.

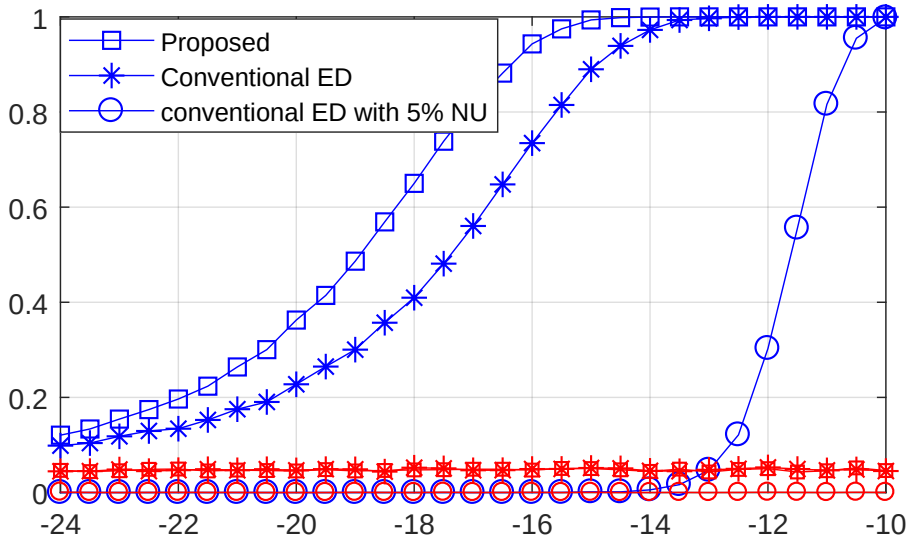

Fig. 11 Performance comparison of the proposed scheme Vs conventional ED scheme with and without NU.

In our experiments, it was observed that the hardware implementation closely followed the accuracy set by the full precision Matlab models, when tested with actual LDACS frame structure. The Matlab and hardware simulation results are given in Fig. 9. A comparison of the detection performance of the proposed scheme and the matched filtering based sensing also shown in the same figure. Though matched filtering offers better detection accuracy at low SNR regions, the higher complexity, and long and variable sensing duration to achieve high accuracy limit the practicality of the scheme. More than that, the matched filtering technique described in [26] is not considered the synchronization issues which is an important concern to maximize SNR.

The advantage of weight optimization is demonstrated in Fig. 10. Same noise variance is considered for the analysis for the i^{th} and $i-1^{th}$ sensing slots. So $w = \frac{1}{2}$ is the optimal weight. The same trend is observed in the simulation results also. we observed that when $w = 1$, (ie, equivalent to conventional ED), a steep drop in the probability of detection compared with $w = 0.5$. It is guaranteed that the performance of the proposed scheme does not fall below the level of conventional ED even if sudden state changes happens in the consecutive sensing intervals. The performance of the proposed scheme is analysed and are compared with the conventional ED for a range of SNRs in Fig. 11. It is observed that the conventional ED performance is highly sensitive to the noise variance uncertainty. A drastic drop of the probability of detection is noticed at $SNR = -10dB$ with 5% NU. The resulting false alarms are also plotted in Fig.11 (red color curves). A deviation from the assumed false alarms has been observed for the case with 5% NU because of the deviation of the threshold from the actual value. The real-time noise variance estimation technique used in this work enhanced the stability against NU. We observed that along with the proposed technique, the conventional

ED also provides reasonable detection accuracy with the proposed noise variance estimation technique.

The various aspects of the performances are analysed and are compared in Fig. 7- Fig.11. These analysis shows that the WEAS with optimised weight effectively separates the two hypotheses ($\mathcal{H}_0$ and $\mathcal{H}_1$) by reducing the effective variance of the test statistic. Also it was perceived that the energy difference incorporated WEAS prevents the performance degradation of regular WEAS when a state change happens. For the optimal w, the SNR wall to get $P_d = 0.9$ & $P_{fa} = 0.1$ is $-16.5dB$ whereas it is $-14.9dB$ for the conventional ED. For achieving better detection accuracy, the proposed method requires only two additional registers to store the previous energy and noise variance values and two additional multipliers to calculate the test statistic and the thresholds. Unlike the proposed scheme, conventional schemes use dedicated hardware for noise variance estimation which effectively reduces overall resource utilization.

Finally, we also validate the performance of the hardware model using simulations in ModelSim. LDACS frames generated in MATLAB were quantised to 16-bit fixed point values, which were mapped into the receiver FIFO in the hardware model for validation. The energy-detection block looks at the FIFO status and reads out samples as soon as it becomes available to start the computation. With frame data available at every clock edge, the sensing logic was able to compute the outcome of sensing (decide between $\mathcal{H}_0$ or $\mathcal{H}_1$) in 10116 cycles. We observe that with 16-bit fixed-point representation for inputs, the hardware implementation offers comparable performance as the MATLAB simulation (see Fig. 9) across all simulation conditions (different SNR conditions). Further, we integrated the design into our radio platform to estimate the resource overheads incurred by the hardware model. Table 2 shows the resource consumption of the radio platform (both transmit and receive chains) after integrating the spectrum sensing logic. The channel filter (transmit path) and channeliser (recieve path) are integrated as reconfigurable modules since only one of them is active at any given time. It can be observed that our state-machine driven approach results in an efficient implementation with very minimal overhead of general purpose resources (1% in Lookup Tables (LUTs), 3% in FlipFlops of the entire device). Also, while the current design consumes 55 DSP blocks, a fully flattened approach would infer 76 additional Digital Signal Processing (DSP) blocks, resulting in over 2× higher DSP resources and energy consumption. The individual building blocks are also extensively pipelined to achieve an operating frequency of 140 MHz in the integrated design. Our results shows that the proposed scheme offers significant improvement in the detection process and can be efficiently deployed in hardware for application in LDACS air-to-ground communication. A comparison of the resource overheads of the proposed scheme, conventional matched filtering, multiplier-less matched filtering, and conventional ED is given in Table 3. Results show that matched filtering offers better detection accuracy more resource overheads. At the same time, the proposed scheme offers better detection accuracy than the conventional ED with comparable resource utilization. While analyzing power consumption, our design consumes a mere 112 mW in operation (dynamic power), with a device static power of 299 mW, compared to the 1038 mW consumed by the matched filter(multiplier-less correlator) [26] based detection scheme, making it an ideal choice for deployment on aircraft onboard systems with limited energy budget. Apart from the resource utilization and power consumption, the

Table 2 Resource utilisation of the Zynq radio platform after integrating the spectrum sensing logic.

Sub-module	FFs	LUTs	BRAMs(36/18)	DSPs
Channel Filter	1,336	1,397	0/0	23
Channeliser	1,581	2,161	4/0	46
Sensing logic	6,179	5,220	0/3	55
RF I/F	22,781	21,970	6/4	77
Reconfig	697	767	1/1	0
Total Utilisation	32,092	30,919	11/8	178
% Utilisation	7.3	14.1	2.75	19.78
Operating Frequency		140 MHz		

Table 3 Resource utilization comparison of the proposed scheme, conventional matched filtering, multiplier-less correlator based matched filtering, and energy detection.

Sensing logic	FFs	LUTs	DSP
Proposed scheme	6179	5220	55
Conventional matched filtering[26]	11968	6112	1500
Multiplier less correlator [26]	24000	29895	0
Conventional ED [7]	6592	12038	48

matched-filter requires a higher sensing period relative to other schemes (as high as up to 58.3 ms) which need to be varied depending on channel conditions, restricting the throughput of the secondary radio. Also, this scheme is not discussing the time synchronization issues associated with the matched filtering, which is an important concern to maximize SNR.

8 Conclusion

In this paper, we proposed a spectrum sensing scheme based on an energy difference incorporated weighted energy averaging for detecting spectral gaps in LDACS communication. The weighted energy averaging helps to reduce the effective variance of the test statistic by adaptively choosing the weights based on current and past energy observations. The scheme also addresses the shortcomings of regular WEAS by incorporating an adaptive energy difference scheme into the WEAS. The technique allows the algorithm to switch between WEAS and conventional ED based on channel state change information derived from the energy difference computation. We show that the proposed scheme offers significant improvement in detection accuracy with more than 90% detection probability even at low SNR conditions and is stable against NU, while incurring less than 3% general purpose resources on a modern FPGA device. In the future, we aim to evaluate the performance of the scheme under multipath fading and shadowing conditions and to improve the robustness of the scheme under such scenarios.

References

1. https://www.faa.gov/nextgen/.
2. https://www.ldacs.com/software/.
3. Single european sky–eurocontrol. http://www.eurocontrol.int/dossiers/single–european–sky
4. Bruno, J. M. and Mark, B. L. (2018). A recursive algorithm for wideband temporal spectrum sensing. *IEEE Transactions on Communications*, 66(1):26–38.
5. Cabric, D., Mishra, S. M., and Brodersen, R. W. (2004). Implementation issues in spectrum sensing for cognitive radios. In *Signals, systems and computers, 2004. Conference record of the thirty-eighth Asilomar conference on*, volume 1, pages 772–776. Ieee.
6. Chin, W. L., Li, J. M., and Chen, H. H. (2016). Low-complexity energy detection for spectrum sensing with random arrivals of primary users. *IEEE Transactions on Vehicular Technology*, 65(2):947–952.
7. Das, S. and Mukhopadhyay, S. (2015). Soc fpga implementation of energy based cooperative spectrum sensing algorithm for cognitive radio. In *2015 6th International Conference on Computers and Devices for Communication (CODEC)*, pages 1–4.
8. Dhabu, S., Vinod, A. P., and Madhukumar, A. S. (2015). Low complexity fast filter bank-based channelization in L-DACS1 for aeronautical communications. In *2015 IEEE 13th International New Circuits and Systems Conference (NEWCAS)*, pages 1–4.
9. Fistas, N. and Phillips, B. (2007). Action plan 17-future communications study-final conclusions and recommendations report. In *Digital Avionics Systems Conference (DASC) Proceedings*, page 12.
10. Ibe, O. (2013). *Markov processes for stochastic modeling*. Newnes.
11. Jacob, P., Madhukumar, A., and Vinod, A. (2015). Efficient aviation spectrum management through dynamic frequency allocation. In *Integrated Communication, Navigation, and Surveillance Conference (ICNS), 2015*, pages L3–1. IEEE.
12. Jin, M., Guo, Q., Xi, J., Li, Y., and Li, Y. (2017). On Spectrum Sensing of OFDM Signals at Low SNR: New Detectors and Asymptotic Performance. *IEEE Transactions on Signal Processing*, 65(12):3218–3233.
13. Lim, Y. C. and Farhang-Boroujeny, B. (1992). Fast filter bank (FFB). *IEEE Transactions on Circuits and Systems II: Analog and Digital Signal Processing*, 39(5):316–318.
14. López-Benítez, M. and Casadevall, F. (2012). Improved energy detection spectrum sensing for cognitive radio. *IET communications*, 6(8):785–796.
15. Ma, Y., Dehnie, S., and Chakravarthy, V. D. (2015). On the near-optimality of training-based glrt spectrum sensing. *IEEE Transactions on Wireless Communications*, 14(9):4894–4906.
16. Mariani, A., Giorgetti, A., and Chiani, M. (2011a). Effects of noise power estimation on energy detection for cognitive radio applications. *IEEE Transactions on Communications*, 59(12):3410–3420.
17. Mariani, A., Giorgetti, A., and Chiani, M. (2011b). Snr wall for energy detection with noise power estimation. In *Communications (ICC), 2011 IEEE International Conference on*, pages 1–6. IEEE.

18. Mathew, L. K. and Vinod, A. (2016). An energy-difference detection based spectrum sensing technique for improving the spectral efficiency of LDACS1 in aeronautical communications. In *Digital Avionics Systems Conference (DASC), 2016 IEEE/AIAA 35th*, pages 1–5. IEEE.
19. Pradhan, H., Kalamkar, S. S., and Banerjee, A. (2015). Sensing-throughput tradeoff in cognitive radio with random arrivals and departures of multiple primary users. *IEEE Communications Letters*, 19(3):415–418.
20. Prawatmuang, W., So, D. K., and Alsusa, E. (2014). Sequential cooperative spectrum sensing technique in time varying channel. *IEEE Transactions on Wireless Communications*, 13(6):3394–3405.
21. Proakis, J. G. (1998). Digital communications fourth edition, 2001.
22. Rugini, L., Banelli, P., and Leus, G. (2013). Small sample size performance of the energy detector. *IEEE Communications Letters*, 17(9):1814–1817.
23. Sajatovic, M., Haindl, B., Ehammer, M., Gräupl, T., Schnell, M., Epple, U., and Brandes, S. (2009). L-DACS1 system definition proposal: Deliverable d2. *Eurocontrol Study Report*.
24. Schnell, M., Epple, U., Shutin, D., and Schneckenburger, N. (2014). LDACS: future aeronautical communications for air-traffic management. *IEEE Communications Magazine*, 52(5):104–110.
25. Shreejith, S., Ambede, A., Vinod, A., and Fahmy, S. A. (2016). A power and time efficient radio architecture for LDACS1 air-to-ground communication. In *Digital Avionics Systems Conference (DASC), 2016 IEEE/AIAA 35th*, pages 1–6. IEEE.
26. Shreejith, S., Mathew, L. K., Prasad, V. A., and Fahmy, S. A. (2018). Efficient spectrum sensing for aeronautical ldacs using low-power correlators. *IEEE Transactions on Very Large Scale Integration (VLSI) Systems*, 26(6):1183–1191.
27. Undertaking, S. J. (2012). European ATM master plan, 2 eds. october 2012. *SESAR Joint Undertaking*.
28. Urkowitz, H. (1967). Energy detection of unknown deterministic signals. *Proceedings of the IEEE*, 55(4):523–531.
29. Wang, J., Chen, Z., Xu, Y., Song, Z., and Chen, R. (2017). Spectrum sensing with random arrivals of primary users by using multiple antennas. In *2017 International Conference on Computer, Information and Telecommunication Systems (CITS)*, pages 190–194.
30. Yucek, T. and Arslan, H. (2009). A survey of spectrum sensing algorithms for cognitive radio applications. *IEEE communications surveys & tutorials*, 11(1):116–130.
31. Zeng, Y. and Liang, Y.-C. (2009). Eigenvalue-based spectrum sensing algorithms for cognitive radio. *IEEE transactions on communications*, 57(6).
32. Zhu, J., Xu, Z., Wang, F., Huang, B., and Zhang, B. (2008). Double threshold energy detection of cooperative spectrum sensing in cognitive radio. In *2008 3rd International Conference on Cognitive Radio Oriented Wireless Networks and Communications (CrownCom 2008)*, pages 1–5.